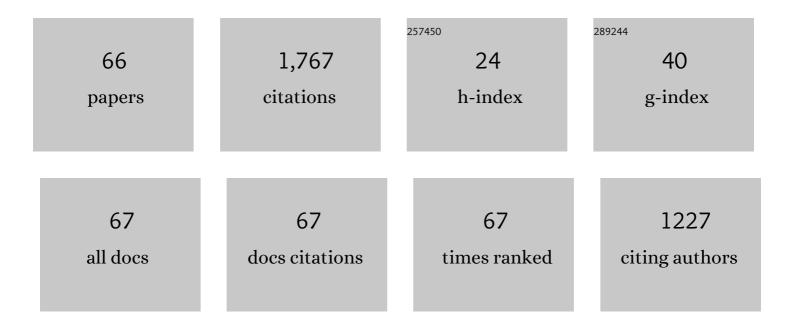
JérÃ'me Yon

List of Publications by Year in descending order

Source: https://exaly.com/author-pdf/4451782/publications.pdf Version: 2024-02-01



#	Article	IF	CITATIONS
1	Droplet size and morphology characterization for dense sprays by image processing: application to the Diesel spray. Experiments in Fluids, 2005, 39, 977-994.	2.4	127
2	Examination of wavelength dependent soot optical properties ofÂdiesel and diesel/rapeseed methyl ester mixture by extinction spectra analysis and LII measurements. Applied Physics B: Lasers and Optics, 2011, 104, 253-271.	2.2	100
3	Review of recent literature on the light absorption properties of black carbon: Refractive index, mass absorption cross section, and absorption function. Aerosol Science and Technology, 2020, 54, 33-51.	3.1	96
4	Comparison of methods to derive morphological parameters of multi-fractal samples of particle aggregates from TEM images. Journal of Aerosol Science, 2012, 47, 12-26.	3.8	86
5	Automated Determination of Aggregate Primary Particle Size Distribution by TEM Image Analysis: Application to Soot. Aerosol Science and Technology, 2014, 48, 831-841.	3.1	86
6	On the radiative properties of soot aggregates part 1: Necking and overlapping. Journal of Quantitative Spectroscopy and Radiative Transfer, 2015, 162, 197-206.	2.3	78
7	Soot optical properties determined by analyzing extinction spectra in the visible near-UV: Toward an optical speciation according to constituents and structure. Journal of Aerosol Science, 2016, 101, 118-132.	3.8	71
8	Effects of multiple scattering on radiative properties of soot fractal aggregates. Journal of Quantitative Spectroscopy and Radiative Transfer, 2014, 133, 374-381.	2.3	66
9	On the radiative properties of soot aggregates – Part 2: Effects of coating. Journal of Quantitative Spectroscopy and Radiative Transfer, 2016, 172, 134-145.	2.3	62
10	Influence of Sampling and Storage Protocol on Fractal Morphology of Soot Studied by Transmission Electron Microscopy. Aerosol Science and Technology, 2010, 44, 1005-1017.	3.1	57
11	Light scattering and absorption by fractal aggregates including soot. Journal of Quantitative Spectroscopy and Radiative Transfer, 2018, 217, 459-473.	2.3	53
12	A simple semi-empirical model for effective density measurements of fractal aggregates. Journal of Aerosol Science, 2015, 87, 28-37.	3.8	50
13	The MERMOSE project: Characterization of particulate matter emissions of a commercial aircraft engine. Journal of Aerosol Science, 2017, 105, 48-63.	3.8	45
14	FracVAL: An improved tunable algorithm of cluster–cluster aggregation for generation of fractal structures formed by polydisperse primary particles. Computer Physics Communications, 2019, 239, 225-237.	7.5	45
15	Revealing soot maturity based on multi-wavelength absorption/emission measurements in laminar axisymmetric coflow ethylene diffusion flames. Combustion and Flame, 2021, 227, 147-161.	5.2	45
16	Characterization of Soot Particles in the Plumes of Over-Ventilated Diffusion Flames. Combustion Science and Technology, 2008, 180, 674-698.	2.3	34
17	Numerical investigation of the possibility to determine the primary particle size of fractal aggregates by measuring light depolarization. Journal of Quantitative Spectroscopy and Radiative Transfer, 2013, 126, 130-139.	2.3	34
18	First in-flight synchrotron X-ray absorption and photoemission study of carbon soot nanoparticles. Scientific Reports, 2016, 6, 36495.	3.3	31

Jérôme Yon

#	Article	IF	CITATIONS
19	Extension of RDGâ€FA for Scattering Prediction of Aggregates of Soot Taking into Account Interactions of Large Monomers. Particle and Particle Systems Characterization, 2008, 25, 54-67.	2.3	30
20	True density of combustion emitted particles: A comparison of results highlighting the influence of the organic contents. Journal of Aerosol Science, 2019, 134, 1-13.	3.8	30
21	Measurement of aggregates' size distribution by angular light scattering. Journal of Quantitative Spectroscopy and Radiative Transfer, 2013, 126, 140-149.	2.3	29
22	A semi-automatic analysis tool for the determination of primary particle size, overlap coefficient and specific surface area of nanoparticles aggregates. Journal of Aerosol Science, 2018, 126, 122-132.	3.8	29
23	Behaviour of aeronautical polymer composite to flame: A comparative study of thermoset- and thermoplastic-based laminate. Polymer Degradation and Stability, 2018, 152, 105-115.	5.8	28
24	Impact of the primary particle polydispersity on the radiative properties of soot aggregates. Proceedings of the Combustion Institute, 2019, 37, 1151-1159.	3.9	24
25	Monte Carlo Aggregation Code (MCAC) Part 2: Application to soot agglomeration, highlighting the importance of primary particles. Journal of Colloid and Interface Science, 2020, 575, 274-285.	9.4	24
26	Original use of a direct injection high efficiency nebulizer for the standardization of liquid fuels spray flames. Review of Scientific Instruments, 2009, 80, 105105.	1.3	21
27	Increase in thermophoretic velocity of carbon aggregates as a function of particle size. Journal of Aerosol Science, 2014, 76, 87-97.	3.8	21
28	Monte Carlo Aggregation Code (MCAC) Part 1: Fundamentals. Journal of Colloid and Interface Science, 2020, 569, 184-194.	9.4	20
29	Impact of necking and overlapping on radiative properties of coated soot aggregates. Aerosol Science and Technology, 2017, 51, 532-542.	3.1	16
30	Influence of primary particle polydispersity and overlapping on soot morphological parameters derived from numerical TEM images. Powder Technology, 2018, 330, 67-79.	4.2	16
31	Investigation of soot oxidation by coupling LII, SAXS and scattering measurements. Combustion and Flame, 2018, 190, 441-453.	5.2	16
32	Specific surface area of combustion emitted particles: Impact of primary particle diameter and organic content. Journal of Aerosol Science, 2019, 137, 105436.	3.8	16
33	Impact of Organic Coating on Soot Angular and Spectral Scattering Properties. Environmental Science & Technology, 2019, 53, 6383-6391.	10.0	16
34	A novel approach for in-situ soot size distribution measurement based on spectrally resolved light scattering. Journal of Quantitative Spectroscopy and Radiative Transfer, 2019, 225, 58-68.	2.3	16
35	Influence of soot aggregate size and internal multiple scattering on LII signal and the absorption function variation with wavelength determined by the TEW-LII method. Applied Physics B: Lasers and Optics, 2015, 119, 643-655.	2.2	15
36	Impact of the competition between aggregation and surface growth on the morphology of soot particles formed in an ethylene laminar premixed flame. Journal of Aerosol Science, 2021, 152, 105690.	3.8	15

Jérôme Yon

#	Article	IF	CITATIONS
37	Impact of the maturation process on soot particle aggregation kinetics and morphology. Carbon, 2021, 182, 837-846.	10.3	15
38	Physicochemical properties of aerosol released in the case of a fire involving materials used in the nuclear industry. Journal of Hazardous Materials, 2015, 283, 340-349.	12.4	14
39	From monomers to agglomerates: A generalized model for characterizing the morphology of fractal-like clusters. Journal of Aerosol Science, 2021, 151, 105628.	3.8	13
40	Time-dependent smoke yield and mass loss of pool fires in a reduced-scale mechanically ventilated compartment. Fire Safety Journal, 2016, 81, 32-43.	3.1	12
41	Experimental investigation of a low Reynolds number flame jet impinging flat plates. International Journal of Heat and Mass Transfer, 2020, 156, 119856.	4.8	12
42	Toxicological impact of organic ultrafine particles (UFPs) in human bronchial epithelial BEAS-2B cells at air-liquid interface. Toxicology in Vitro, 2022, 78, 105258.	2.4	12
43	Clogging of Industrial High Efficiency Particulate Air (HEPA) Filters in Case of Fire: From Analytical to Large-Scale Experiments. Aerosol Science and Technology, 2014, 48, 939-947.	3.1	11
44	On the use of PIV, LII, PAH-PLIF and OH-PLIF for the study of soot formation and flame structure in a swirl stratified premixed ethylene/air flame. Proceedings of the Combustion Institute, 2021, 38, 1851-1858.	3.9	11
45	Design and performance of a new device for the study of thermophoresis: The radial flow thermophoretic analyser. Journal of Aerosol Science, 2013, 61, 1-12.	3.8	10
46	Analysis of the Soot Particle Size Distribution in a Laminar Premixed Flame: A Hybrid Stochastic/Fixed-Sectional Approach. Flow, Turbulence and Combustion, 2020, 104, 753-775.	2.6	10
47	Development of a standardized in vitro approach to evaluate microphysical, chemical, and toxicological properties of combustion-derived fine and ultrafine particles. Journal of Environmental Sciences, 2022, 113, 104-117.	6.1	10
48	In-situ characterization of nanoparticle beams focused with an aerodynamic lens by Laser-Induced Breakdown Detection. Scientific Reports, 2015, 5, 15696.	3.3	9
49	Horizontal Planar Angular Light Scattering (HPALS) characterization of soot produced in a laminar axisymmetric coflow ethylene diffusion flame. Combustion and Flame, 2021, 232, 111539.	5.2	9
50	Influence of the dry aerosol particle size distribution and morphology on the cloud condensation nuclei activation. An experimental and theoretical investigation. Atmospheric Chemistry and Physics, 2020, 20, 4209-4225.	4.9	8
51	Spectral Study of the Smoke Optical Density in Non-flaming Condition. Procedia Engineering, 2013, 62, 821-828.	1.2	7
52	Chemical discrimination of the particulate and gas phases of miniCAST exhausts using a two-filter collection method. Atmospheric Measurement Techniques, 2020, 13, 951-967.	3.1	7
53	Black carbon aerosol number and mass concentration measurements by picosecond short-range elastic backscatter lidar. Scientific Reports, 2022, 12, 8443.	3.3	7
54	Contribution to the study of particle resuspension kinetics during thermal degradation of polymers. Journal of Hazardous Materials, 2013, 250-251, 298-307.	12.4	6

Jérôme Yon

#	Article	IF	CITATIONS
55	Spectrally resolved light extinction enhancement of coated soot particles. Atmospheric Environment, 2018, 186, 89-101.	4.1	6
56	Morphological and radiative characteristics of soot aggregates: Experimental and numerical research. Scientific Reports, 2020, 10, 411.	3.3	6
57	Soot and velocity mapping and 2D soot sheet dimensions in a buoyant wall-fire. Proceedings of the Combustion Institute, 2017, 36, 3219-3226.	3.9	5
58	Assessing the limits of Rayleigh–Debye–Gans theory: Phasor analysis of a bisphere. Journal of Quantitative Spectroscopy and Radiative Transfer, 2021, 264, 107550.	2.3	5
59	Application of planar auto-compensating laser-induced incandescence to low-sooting turbulent flames and investigation of the detection gate width effect. Aerosol Science and Technology, 2021, 55, 1215-1229.	3.1	5
60	A STATISTICAL MORPHOLOGICAL DETERMINATION OF THE GROWTH RATE OF THE INTERFACIAL DISTURBANCE OF AN EXCITED RAYLEIGH JET;. Journal of Flow Visualization and Image Processing, 2004, 11, 239-256.	0.5	2
61	Measurement of the Mass Specific Extinction Coefficient of Acetylene, Toluene and Polymethyl Methacrylate Soot Particles in Visible and Near-Infrared Wavelengths. Fire Safety Science, 2008, 9, 231-240.	0.3	2
62	A semi-empirical correction for the Rayleigh-Debye-Gans approximation for fractal aggregates based on phasor analysis: Application to soot particles. Journal of Quantitative Spectroscopy and Radiative Transfer, 2022, 283, 108143.	2.3	2
63	Comprehensive characterization of sooting butane jet flames, Part 2: Temperature and soot particle size. Combustion and Flame, 2021, 233, 111596.	5.2	1
64	Feasibility of Particle Imaging Velocimetry in Cone Calorimeter experiments. Fire Safety Science, 2014, 11, 152-164.	0.3	1
65	Soot Volume Fraction Measurements by Auto-Compensating Laser-Induced Incandescence in Diffusion Flames Generated by Ethylene Pool Fire. Frontiers in Mechanical Engineering, 2021, 7, .	1.8	1
66	Comparison and Assessment of Particle Mass Concentration Measurements in Fire Smokes with a Microbalance, Opacimeter and PPS Devices. , 2017, , 735-742.		0